



Influence of Chemoautotrophic Organic Carbon on Sediment and Its Infauna in the Vicinity of the Rainbow Vent Field

Reyhaneh Roohi^{1*}, Ragna Hoogenboom¹, Ronald Van Bommel², Marcel T. J. Van Der Meer², Furu Mienis¹ and Sabine Gollner¹

¹ Department of Ocean Systems, Royal Netherlands Institute for Sea Research (NIOZ), Texel, Netherlands,

² Department of Marine Microbiology and Biogeochemistry, Royal Netherlands Institute for Sea Research (NIOZ), Texel, Netherlands

OPEN ACCESS

Edited by:

Jozee Sarrazin,
Institut Français de Recherche pour
l'Exploitation de la Mer (IFREMER),
France

Reviewed by:

Travis William Washburn,
Geological Survey of Japan (AIST),
Japan
Xikun Song,
Xiamen University, China

*Correspondence:

Reyhaneh Roohi
reyhane.roohi@gmail.com

Specialty section:

This article was submitted to
Deep-Sea Environments and Ecology,
a section of the journal
Frontiers in Marine Science

Received: 29 June 2021

Accepted: 13 May 2022

Published: 13 June 2022

Citation:

Roohi R, Hoogenboom R, Van
Bommel R, Van Der Meer MTJ,
Mienis F and Gollner S (2022) Influence
of Chemoautotrophic Organic Carbon
on Sediment and Its Infauna in the
Vicinity of the Rainbow Vent Field.
Front. Mar. Sci. 9:732740.
doi: 10.3389/fmars.2022.732740

Hydrothermal vents have been recognised as isolated islands of productivity in the deep sea, but very little is known about the transport and export of chemoautotrophic produced organic carbon to vent surrounding habitats. Here, we investigate vent carbon export and its influence on benthic food webs in sediments at the Rainbow (RB) vent field at the Mid Atlantic Ridge in ~2200 m water depth. Two sites were considered along the dispersal direction of the RB vent plume for sample collection: the close vicinity at about ~30-100 m ("near-vent"); and at 4 km distance ("off-vent") to the nearest venting area. At both sites, box corers were used to sample sediments and their fauna. A turbidity sensor mounted on a CTD/Rosette provided data on the presence of a vent fluid plume in the water column. Niskin bottles were used to sample suspended particulate organic matter (SPOM) from the plume, as well as from surface waters at 75 m depth. SPOM, sediments and fauna were analysed for nitrogen and carbon stable isotopes. Carbon derived from *in situ* chemoautotrophy, characterised by depleted $\delta^{13}\text{C}$, was taken up by infauna close to the venting area as the main nutrition source, while fauna at the off-vent site showed less depleted $\delta^{13}\text{C}$ with a signature more typical for photosynthetic-derived material. Nematodes were the most abundant faunal taxon. Their abundance and biomass were variable and not different at the two studied sites. *In situ* derived organic matter was traced back in the food web in the close vicinity of the venting area. The connectivity of vent and non-vent habitats should be taken appropriately into account when designing future spatial management plans with regard to deep-seabed mining at hydrothermal vents.

Keywords: hydrothermal vent, deep-sea sediment, plume, connectivity, trophic interaction, isotopes, fauna, organic carbon

1 INTRODUCTION

It has only recently been recognized that deep-sea vents are not isolated ecosystems, but also influence the surrounding areas (Levin et al., 2016). Deep-sea vent plumes transport vent larvae (Adams et al., 2012; Kim et al., 2015) and export nutrients and trace metals to the vent surroundings, influencing the microbial community composition in the water column

(Haalboom et al., 2020). Faunal communities on hard substrates in the vent surroundings harbor a mix of typical “vent” meiofaunal species (e.g. *Dirivultid* copepods) and of species/genera known from coastal areas and deep-sea sediments (Gollner et al., 2010; Gollner et al., 2015; Gollner et al., 2020), and show increased functional diversity (Alfaro-Lucas et al., 2020). Benthic species composition in sediments surrounding Rainbow is different compared to control deep-sea sediments and highly influenced by the vent plume’s fall out (Klunder et al., 2020). Nematode community composition in sediments in the surroundings of Snake Pit and TAG vent fields on the Mid-Atlantic Ridge is hypothesized to be influenced by geochemical setting and food availability (Spedicato et al., 2020). A study in the northern West-Pacific, suggested that the effect of *in situ* derived organic matter as a food source near vents may be limited to at most several 100 m away from the venting area (Nomaki et al., 2019). Overall, very little is known about the role of vent *in situ* derived organic matter on food web and community composition in the vent surroundings.

The importance of understanding the interactions of vents with their surroundings is growing, as the potential for disturbances in the form of deep-seabed mining rises. Hydrothermal vent ecosystems are typically rich in seafloor massive sulfides and there is globally a growing interest to mine these minerals in the future (Dover, 2011; Boschen et al., 2013; Dover et al., 2018). Some countries have already tested mining or plan mining-tests in their national waters (Collins et al., 2013; Boschen et al., 2015), and to date, 7 exploration contracts for seafloor massive sulfide mining have been issued by the International Seabed Authority (ISA) in areas beyond national jurisdiction (www.isa.org.jm). Mining will have impacts on the environment, including for example removal of habitat or the creation of sediment plumes (Gollner et al., 2017). The ISA is currently working on the development of Regional Environmental Management Plans, which shall include mitigation actions, such as areas to be protected from seabed mining (ISA, 2019). Understanding the extent of vent influence and ecological connectivity to the surrounding environment are needed to ensure proper mitigation actions for human disturbances, and to border marine protected areas in the deep sea.

One form of determining the geographical size or “footprint” of an ecosystem includes the detection of trophic links within and between ecosystems. Food web studies can use stable isotopes of carbon and nitrogen to detect the sources of the production, and define the trophic level, by comparing the ratio of the heavier to lighter isotopes (Griffin and Valiela, 2001; Govenar, 2012). Analyzing nitrogen and carbon stable isotopes allows the establishment of trophic interactions between species (Pinnegar and Polunin, 2000). At hydrothermal vents, there are different potential food sources with different $\delta^{13}\text{C}$ ratios including (1) photosynthetically derived organic matter from the sea surface (-24‰ to -22‰), (2) chemo-autotrophs that fix carbon through sulfide oxidation based on Calvin-Benson-Bassham (CBB) cycle (-36‰ to -30‰), (3) chemo-autotrophs that fix carbon through sulfide oxidation based on reductive tricarboxylic acid (rTCA) cycle (-15‰ to -10‰) and (4) methanotrophs (-19 ± 3.5‰ at Rainbow (RB) vent) (Portail

et al., 2018 and references therein). Therefore, the $\delta^{13}\text{C}$ signature can be used to identify which organic carbon sources (chemo- or photosynthetic) fauna in the vent surrounding rely on.

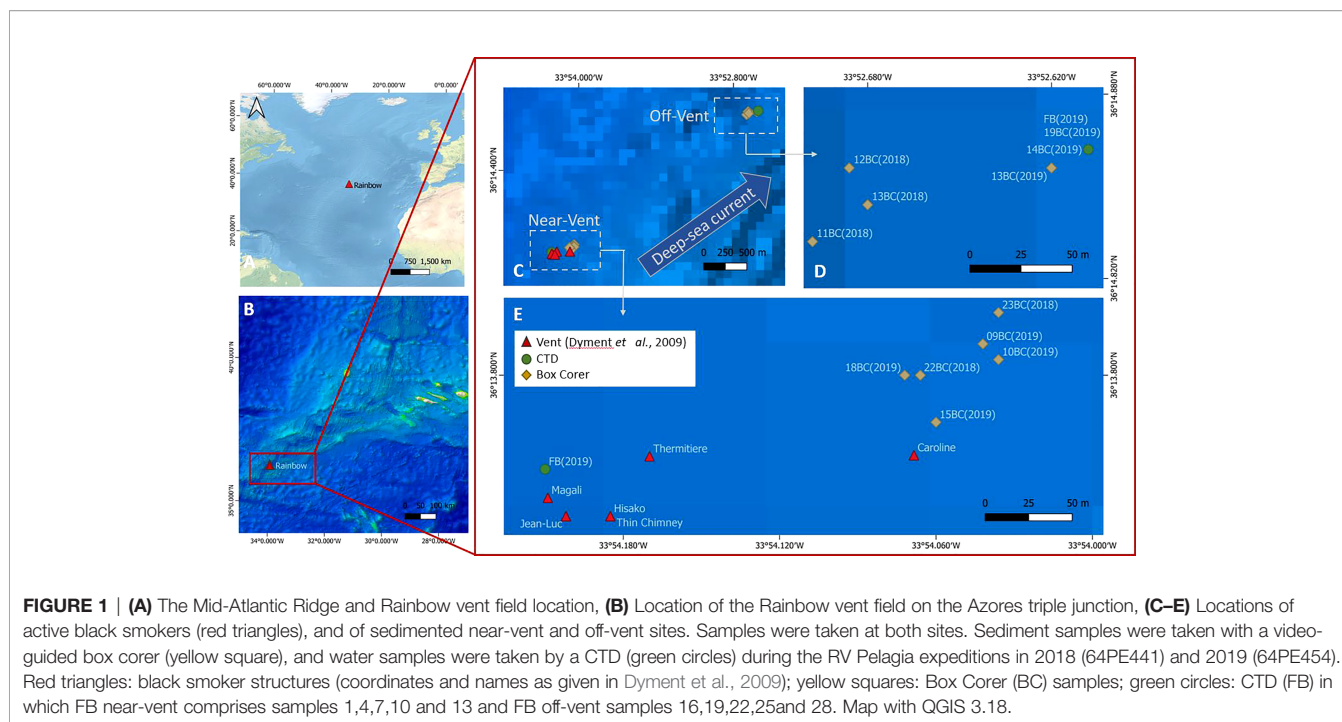
The RB vent produces one of the most persistent and strongest plumes on the Mid-Atlantic Ridge (MAR, German et al., 1996; Thurnherr and Richards, 2001), making it a good location to explore the extent of *in situ* produced organic matter export to vent surroundings. The RB vent field (36°149N, 33°549W, ~2250 m depth) was discovered in 1996 on the Azores triple junction (ATJ) along the MAR (German et al., 1996) (**Figure 1A**). It is located at a slow-spreading ridge with a spreading rate of approximately 21.5 mm yr⁻¹ (Andreani et al., 2014). At least ten black smokers eject the plume that is rising up to 200 m above the vent field and is dispersed predominantly to the north and east of the source with an average current speed of 5-6 cms⁻¹ (Thurnherr and Richards, 2001; Thurnherr et al., 2002; Edmonds and German, 2004). The vent fluid dispersal is controlled by the variation of vent emission and deep-sea current direction which is following the contours of the rift valley and can be detected up to 50 km away from the vent site (Khripounoff et al., 2001; Edmonds and German, 2004; Haalboom et al., 2020). The plume is enriched in trace metals in which the composition changes as it is aged and dispersed, it has very low concentrations of organic carbon and is characterized by the presence of chemoautotrophic microbial communities (Khripounoff et al., 2001; Edmonds and German, 2004; Haalboom et al., 2020).

The fauna living on/very close to black smokers at the RB vent field is relatively well known and characterized by small mussel beds and shrimp swarms, with associated species such as *Amathys lutzi* or spionid polychaetes (Desbruyères et al., 2000; Desbruyères et al., 2001; Portail et al., 2018). Portail et al. (2018) studied the food web complexity at the RB vent. However, there is no knowledge of food webs in vent surrounding areas, and very limited knowledge on the taxonomic composition of sediment infauna, with metabarcoding revealing that their composition is influenced by the RB vent plume’s fall out (Klunder et al., 2020). Here, we investigate the ecological “footprint” of the RB vent field, i.e., the export of *in situ* produced organic carbon and its importance as a potential food source for faunal communities living in the sediments in the vent surrounding areas. Along the dispersal direction of the plume, water column and sediment samples were collected at two sites: near-vent (~30-100 m distance from RB black smokers) and off-vent (4 km away from RB). We analysed the organic matter content, carbon and nitrogen stable isotopes of suspended particulate organic matter (SPOM) in the water column, and of sediments and fauna living in the sediments. In addition, we analysed faunal abundance and biomass of nematodes, the dominant taxon in the sediments.

2 MATERIAL AND METHODS

2.1 Sampling

The sampling sites were chosen based on preliminary studies of plume dispersal by Haalboom et al. (2020), and based on exact



coordinates of RB vent smokers by Dyment et al. (2009). Samples were obtained during two research expeditions with RV Pelagia during cruise 64PE441 (16th to 25th of June 2018) and 64PE454 (24th of June to 4th of July 2019). Sediment cores and water samples were collected at two sites downstream of the plume: very close to the vent at approximately 30–100 m distance from the nearest black smoker (near-vent) and at ~4 km distance from the vent (off-vent) (Figures 1B–E and Table S1). A NIOZ-designed video-guided stainless steel cylindrical box corer (inner diameter 50 cm and 55 cm height), a trip valve sealing the box, was used to obtain quantitative sediment samples. The camera was used to avoid sampling hard substrates. In practice, the box corer was (1) lowered towards the bottom until the bottom became visible, (2) the ship with the box corer was moved into position, (3) the box corer was lifted several meters upwards to gain enough speed, (4) the box corer was deployed, resulting in ~30 cm deep penetration into the sediment with ~10–20 cm of overlying bottom water in the box corer. After the box corer was on deck, it was inspected for sampling success (i.e. enough overlying bottom-water; no leaking due to underlying rocks in sediments that had caused deformation of the box corer or incomplete closure). Only successfully retrieved box corers were subsampled with push cores. For all meiofaunal analyses, push cores with a ~5 cm diameter (area of 19.63 cm²) were used. For higher taxon diversity and nematode biomass analyses, the top 10 cm of each push core was fixed in a 4% buffered formaldehyde solution. For faunal stable isotope analyses, the top 10 cm of the push cores were frozen at -20°C, but only the top 5 cm have been analysed. One retrieved box corer (23BC) contained only a 7 cm thick sediment layer due to the hard substrate below. In addition to 5 cm diameter push cores, plastic syringes with 3 cm

diameter (area of 7.07 cm²) were pushed into the sediment and frozen at -20°C for bulk sediment stable isotope analyses back in the lab.

Water samples were collected with a CTD/Rosette, at the same locations as the sediment samples. 12-liter Niskin bottles were closed at approximately 2000 m water depth, with 4 samples collected at different depths in the maximum deep-water turbidity layer, indicative for the presence of the hydrothermal plume. In addition, one sample was collected in the chlorophyll maximum layer at 75 m water depth (Figure 2). For SPOM analyses, 2x10 L of water from each water depth were filtered over pre-weighed and pre-combusted GFF filters on board, rinsed with a minimum amount of MilliQ water to remove salt, and stored at -20°C (Table S1).

2.2 TOC, $\delta^{13}\text{C}$ and $\delta^{15}\text{N}$ Analyses of Water and Sediment Samples

The SPOM filters were decalcified before C and N stable isotope analyses. In total 10 SPOM filters were analysed; 5 from near-vent and 5 from off-vent. One sample (FB10) from the near-vent plume did not have enough material to measure the N stable isotope signature, even though the complete filter was analysed. The filters were moistened with some drops of double-distilled water (bidest) and were placed in a chamber filled with HCl gas overnight, followed by drying in an oven at 60°C. Each SPOM filter was manually folded and compacted in a tin capsule. The C and N isotope ratios for SPOM filters were measured in a single analytical run, and certified isotope standards acetanilide (0.3–0.6 mg), casein (0.2–0.5 mg) and urea (0.3–0.8 mg) were used as reference standards.

A total of 7 sediment cores, 4 from near-vent and 3 from off-vent, were analysed at 1 cm intervals until 5 cm core depth

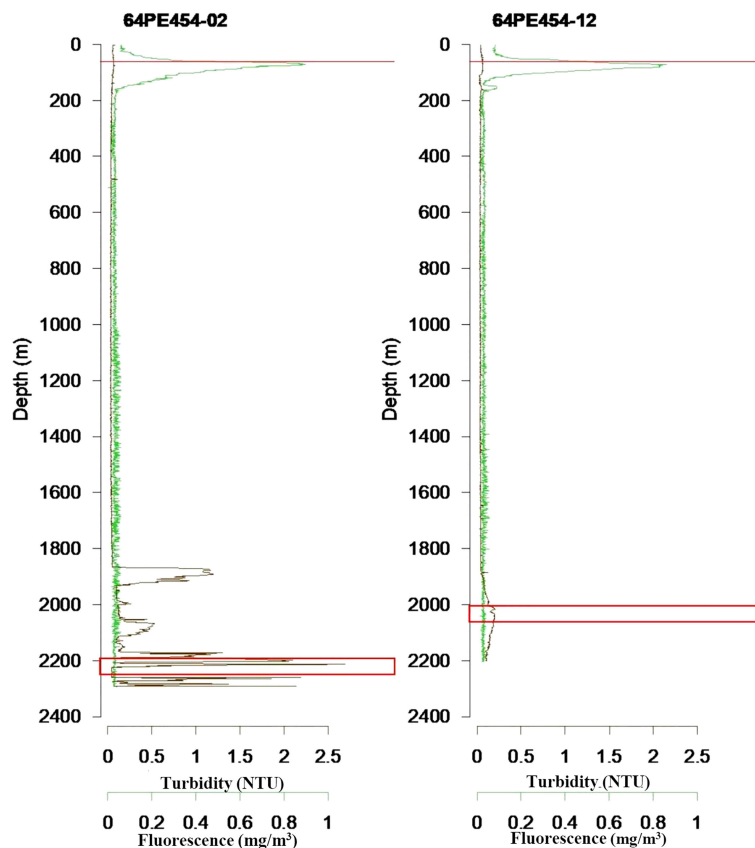


FIGURE 2 | Turbidity and fluorescence profiles in near-vent site (64PE454-02) and off-vent site (64PE454-12) water column. The maximum turbidity in deep water represents the vent plume. The sampling depths are marked with a red line at 75 m water depth, and red squares around 2000 m water depth.

(Table S1). The sediment samples were freeze-dried and ground to a fine and homogeneous powder. This powder was used for $\delta^{15}\text{N}$ and $\delta^{13}\text{C}$ analyses. For $\delta^{13}\text{C}$ analyses, the powder was decalcified to remove inorganic carbon. Sediments were decalcified in Borosilicate glass culture tubes with 2M HCL added in drops until no reaction (bubbling) was visible. The tubes with sediments were shaken for 500 minutes in a table shaker and were afterward centrifuged at 2000 RPM for 5 minutes. After centrifugation, to remove acid from the decalcified samples, the liquid above the sediment was carefully removed with a pipet, and 1 ml doubly distilled water (Bidest) was added to the sediments in the tubes and vortexed until the sediments were resuspended and mixed well with water; followed by adding approximately 10 ml Bidest water to fill up the tube. The centrifugation and removing liquid process were repeated until the pH of the remaining liquid above the sediment in tubes was higher than 5, after which the decalcified samples were freeze-dried. All sediment samples were weighed precisely in tin capsules to carry out stable isotope analysis (SIA). The capsules were crimped and manually compacted to minimize internal air space. Great care was made to avoid any contamination with solvents, fingers and dust. Certified standards comprised 0.05-0.12 mg Benzoic acid and Acetanilide to measure $\delta^{13}\text{C}$, and

Acetanilide (0.5-0.8 mg), Casein (0.3-0.8 mg) and Urea (0.3-0.8 mg) to measure $\delta^{15}\text{N}$.

All values for stable isotope analyses are expressed in δ (‰) notation with respect to the PeeDee Belemnite ($\delta^{13}\text{C}$), and Air ($\delta^{15}\text{N}$) because of the constant average abundance of ^{15}N (Kendall and Caldwell, 1998), in which $\delta^{\text{HX}} = [(R_{\text{SAMPLE}}/R_{\text{STANDARD}} - 1)] \times 10^3$, where R is $^{13}\text{C}/^{12}\text{C}$ or $^{15}\text{N}/^{14}\text{N}$ (Fry, 2006). The stable isotope composition ($\delta^{13}\text{C}$ and $\delta^{15}\text{N}$) of all samples was measured using a Flash 2000 (Organic Elemental Analyzer) MAS 200 autosampler that was connected *via* CONFIO IV to DELTA V ADVANTAGE (isotope ratio mass spectrometer (IRMS)) and ISODAT 3.0 Gas Ratio MS Software was used. The total organic carbon (TOC) was measured along with carbon and nitrogen stable isotope ratios and the TOC (%) calculation was based on the MS-signal. To test the relationships of TOC, $\delta^{13}\text{C}$ and $\delta^{15}\text{N}$, biplots of linear regression were created and the Pearson's correlation coefficient r and p -values calculated.

2.3 Stable Isotope Analyses of Meiofauna

We used 4 box cores (12 push cores) from near-vent and 3 box cores (9 push cores) from off-vent to measure stable C and N isotope values of meiofauna (Table S2). For meiofauna

extraction, sediment samples were thawed and rinsed with 32 μm -filtered tap water through 1 mm and 32 μm mesh sieves. The remaining sediments on the 32 μm sieve were put into centrifugation tubes. For centrifugation of sediments, colloidal silica polymer was used as the flotation medium (H.C. Stark, Levasil 200/40%, $q = 1.17$) and kaolin was used to hold back the heavier particles during decantation (Holme and McIntyre, 1971). Each sample was centrifuged 3 times for 6 minutes at 3500 rpm. The flotation medium with animals was passed through a 32 μm sieve, rinsed with Milli-Q water, and meiofauna transferred into petri dishes. A stereomicroscope was used to identify meiofauna to higher taxonomic levels (i.e. nematodes, copepods, polychaetes) based on Higgins and Thiel (1988) and Giere (2009). For reliable detection of C and N compositions, the minimum required weight for meiofauna is 0.1 mg (Portail et al., 2018) which is estimated around 300 copepods or nematodes (Lebreton et al., 2012). Meiofaunal individuals were hand-picked under a stereomicroscope and pooled per higher taxon directly into a tin capsule. The total number of individuals per taxon extracted from near-vent was 502 nematodes, 121 copepods, 12 polychaetes and 711 nematodes and 80 copepods for off-vent. No polychaetes were found at this site. Although meiofauna was completely sampled from the sediment samples, there was not enough material to reliably measure $\delta^{15}\text{N}$ values of meiofauna and for the off-vent site, not even enough for a $\delta^{13}\text{C}$ value for copepods. Tin capsules with animals were freeze-dried, weighed and measured on the Flash 2000 (Organic Elemental Analyzer; see above). Certified isotope standards acetanilide (0.01-0.1 mg), casein (0.015-0.12 mg) and urea (0.03-0.3 mg) were used as the reference standards for $\delta^{13}\text{C}$.

2.4 Abundance and Biomass Analyses of Nematodes

In addition to the higher meiofaunal taxa counts obtained whilst picking fauna for stable isotopes analyses (from 21 push cores; see *Meiofauna Abundance, Biomass and Isotope Values*), we analyzed higher meiofaunal taxa, and nematode biomass from additional 9 push cores (Table S2). In total, 30 push cores (from

12 box corers) were compared for meiofaunal abundance, 16 push cores from near-vent and 14 push cores from off-vent. Biomass data were based on 4 push cores from near-vent and 5 push cores from off-vent (see Table S2).

Biomass was only calculated using non-damaged individuals (81% of specimens near-vent and 79% of specimens off-vent) as required in the formula described by Andrassy (1956). The statistical analysis is based on standardized data for a 10 cm^2 area. The difference in the abundance and biomass of meiofauna near-vent and off-vent was analyzed by applying Welch's t-test (unequal variances t-test).

To extract meiofauna used for biomass analyses from the sediments, formaldehyde from sediment samples was removed, and sediments were centrifuged as described in 3.3. to extract fauna. A stereomicroscope was used to count and identify meiofauna to higher taxonomic levels (i.e. nematodes, copepods, polychaetes) based on Higgins and Thiel (1988) and Giere (2009). Nematodes were mounted on glass slides, by placing them first into a solution of water/ethanol/glycerol (61/35/4) followed by evaporation for 2 days in a 40°C oven. Afterwards, nematodes were placed into a drop of glycerin on a glass slide, covered with a glass slip and sealed with lacquer (Higgins and Thiel, 1988). The biomass of nematodes was calculated by measuring individual's dimensions and according to $WW (\mu\text{g}) = (L \times W^2) / Cf$ (Andrassy, 1956), where $L (\mu\text{m})$ is the nematode's length, $W (\mu\text{m})$ is its width at the widest point and Cf is 1.6×10^6 as the conversion factor.

3 RESULTS

3.1 $\delta^{13}\text{C}$ and $\delta^{15}\text{N}$ of SPOM

The $\delta^{13}\text{C}$ signature of SPOM collected in the plume was depleted and similar at the near-vent ($-26.33 \pm 1.12\text{‰}$) and off-vent ($-26.22 \pm 0.31\text{‰}$). $\delta^{13}\text{C}$ signatures of SPOM from surface water samples (75 m water depth) at near-vent and off-vent were -23.14‰ and -22.60‰ , respectively (Table 1 and Figure 6). Samples from the near-vent had a lower $\delta^{15}\text{N}$ value (average 2.4‰), compared to the off-vent sample (average 6‰).

TABLE 1 | The $\delta^{13}\text{C}$ and $\delta^{15}\text{N}$ of SPOM filters within the plume close to Rainbow vent (near-vent; between 2190 and 2291 m depth) and at 4 km distance to the vent (off-vent; between 1933 and 2202 m depth).

Site	Filter Name	Water Depth (m)	Volume (ml)	Turbidity (NTU)	$\delta^{13}\text{C}$ (‰)	$\delta^{15}\text{N}$ (‰)
Near-Vent	FB1	2291	4000	5.72	-26.23	2.49
	FB4	2285	4750	9.76	-27.59	2.87
	FB7	2260	4250	2.00	-25.20	4.86
	FB10	2190	8500	0.40	-27.39	NA
	FB13	75	8500	0.05	-23.14	-0.23
Off-Vent	FB16	2202	8175	0.08	-25.83	7.05
	FB19	2140	8000	0.12	-26.44	4.82
	FB22	2051	8500	0.20	-26.48	5.61
	FB25	1933	8050	0.09	-26.13	6.36
	FB28	75	9050	0.05	-22.60	3.67

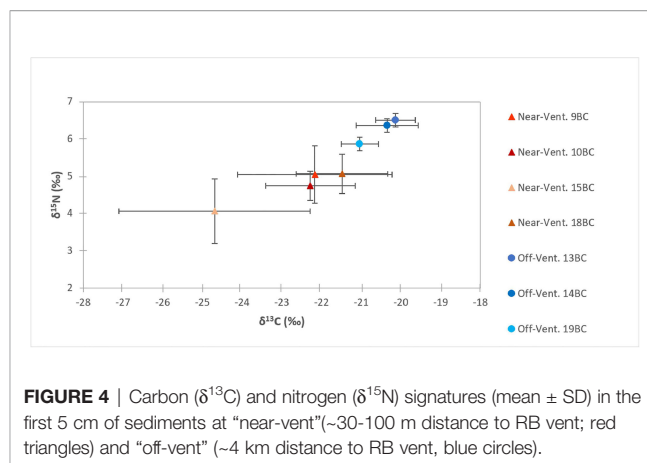
In addition, $\delta^{13}\text{C}$ ratio of SPOM filters was analysed from surface water samples at 75 m depth. Site, sample name (filter number), sampling depth, volume of the filtered water, turbidity at the location, and delta values of carbon and nitrogen stable isotopes are given. NA, Not Available.

3.2 TOC, $\delta^{13}\text{C}$ and $\delta^{15}\text{N}$ in Sediment Samples

Surface sediment TOC concentrations of near-vent sediment samples ($0.50\% \pm 0.16$) were ~ 2.5 times higher than off-vent samples ($0.16\% \pm 0.03$). **Figure 3** shows the vertical profile of TOC, $\delta^{13}\text{C}$ and $\delta^{15}\text{N}$ based on the mean and two standard deviations. Near-vent, the top 2 cm had an average TOC content of 0.50%, which was decreasing to 0.26% in 2 to 5 cm depth. Off-vent, no variation in TOC (average 0.16%) was observed with depth. The average $\delta^{13}\text{C}$ value in the first cm in near-vent sediments (-24.6‰) was lower than for the first cm in off-vent sediments (-21.1‰). $\delta^{13}\text{C}$ values in near-vent sediments increased with depth (-20.8‰ at 5 cm depth), but remained rather similar off-vent (-20.4‰ at 5 cm depth). A similar trend was observed for $\delta^{15}\text{N}$ with values increasing with depth from 4 to 5.4 ‰ near-vent and rather similar $\delta^{15}\text{N}$ values from 6.1 to 6.3 ‰ off-vent. In the sediment samples at the near-vent site, C and N isotopes showed a heterogeneous pattern: the $\delta^{13}\text{C}$ varied between -26.7‰ to -20.2‰ , and $\delta^{15}\text{N}$ from 3.2 ‰ to 5.9 ‰, while there was little variation in the sediments from off-vent, for both $\delta^{13}\text{C}$ value (-21.7‰ to -19.6‰) and $\delta^{15}\text{N}$ (5.6 ‰ to 6.7 ‰) (**Figures 3B, C, 4**). However, a significant correlation was found between $\delta^{13}\text{C}$ and TOC ($r^2 = 0.84$, $p < 0.001$), $\delta^{15}\text{N}$ and TOC ($r^2 = 0.84$, $p < 0.001$) when considering all sediment samples (**Figure 5**).

3.3 Meiofauna Abundance, Biomass and Isotope Values

Meiofaunal abundance was similar near-vent (mean 35.69 ± 28.78 per 10 cm^2) and off-vent (mean 33.20 ± 16.20 per 10 cm^2) (p -value: 0.86). Nematodes dominated the communities with 13 to 83 ind. 10 cm^{-2} near-vent and with 14 to 51 ind. 10 cm^{-2} off-vent. Mean individual nematode biomass was very variable and no statistic difference was detected between “near-vent” ($0.50 \pm 3.93 \mu\text{g}$) and off-vent ($0.93 \pm 4.35 \mu\text{g}$) ($p = 0.72$) (**Table 2**). Mean biomass per 10 cm^{-2} was also variable ($30.68 \pm 25.81 \mu\text{g}$ near-vent; $20.05 \pm 16.31 \mu\text{g}$ off-vent; $p = 0.22$). The second most abundant taxon were copepods with <1 to 8 ind. 10 cm^{-2} near-vent, and 1 to 7 ind. 10 cm^{-2} off-vent. Polychaetes, the only macrofaunal taxon observed, were only detected near-vent (**Table 3**).

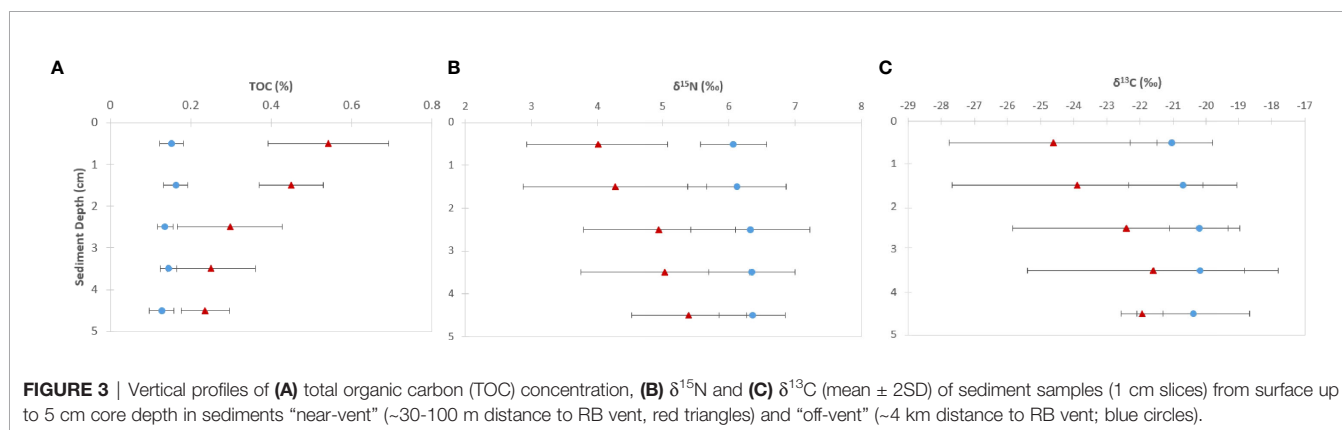


Comparing the $\delta^{13}\text{C}$ values of nematodes living in the near-vent (-28‰) and the off-vent (-22‰) sediments, depleted values were found in near-vent sites (**Figure 6**). Near the vent, different $\delta^{13}\text{C}$ values were detected for nematodes (-28.2‰), copepods (-26.1‰) and polychaetes (-24.9‰). The $\delta^{13}\text{C}$ values of meiofauna measured in our study and other studies are provided in **Table 4**.

4 DISCUSSION

4.1 Vent Fluid Associated Organic Carbon Input to the Surrounding Sediments

The hydrothermal plume supplies a potential carbon source in addition to the photosynthetically derived organic matter in the vicinity of the RB vent, which is supported by depleted stable carbon isotope values of SPOM collected within the plume and in the surface sediments near the vent. Plumes are typically rich in free-living sulfur oxidizing and methanotrophic microbes and represent biogeochemical hotspots for carbon fixation in the dark ocean (Mattes et al., 2013). Concentrations of dissolved and particulate organic carbon are elevated in buoyant plume samples (Bennett et al., 2011), and the primary carbon production (chemosynthetic organic carbon) in hydrothermal plumes has been estimated to be at least 2.0 mg C l^{-1} at EPR 21°N



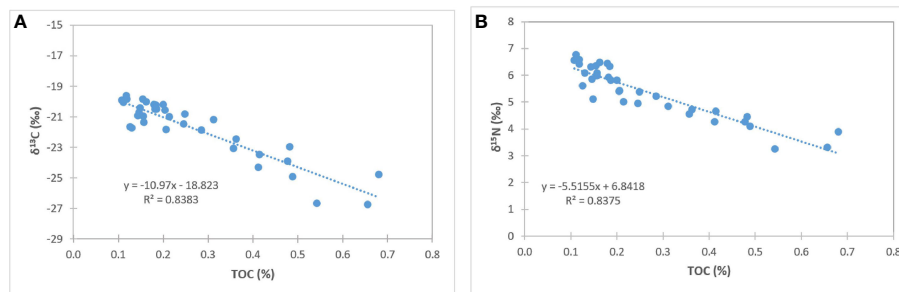


FIGURE 5 | Correlation of $\delta^{13}\text{C}$ and TOC (A), and $\delta^{15}\text{N}$ and TOC (B) concentrations in sediments near-vent and off-vent.

vent fluid (McCullom, 2000). The high fluid fluxes and higher concentration of chemoautotrophic microbes within the plume in the direct vicinity of the vent and to a limited extent also further away may thus provide chemosynthetic TOC to the vent surrounding pelagic environment (Portail et al., 2018; Haalboom et al., 2020).

Total organic carbon in surface sediments was higher near-vent ($0.49\% \pm 0.16$) than off-vent ($0.15\% \pm 0.03$), suggesting that plume fall out and impact is higher in near-vent areas. Our results are in accordance with findings at vents near Japan located in the Izu-Ogasawara Arc of the western North Pacific, where TOC in sediments at the direct base of the chimney was higher compared to sediments further away from the vent (Nomaki et al., 2019). The reduction of TOC with distance to the RB vent may be closely linked to the observed reduction of plume intensity with distance as shown by a decrease in turbidity with increasing distance to the vent plume source, the chimneys (Haalboom et al., 2020) (Figure 2).

Near-vent, $\delta^{13}\text{C}$ sediment values were very variable and more depleted ($\sim -25\text{‰}$) at the sediment surface (0-1 cm) and less depleted at 5 cm sediment depth ($\sim -21\text{‰}$), showing prominent input of chemosynthetically derived organic carbon from the plume ($\sim -26\text{‰}$) to the surface sediments. The heterogeneity in $\delta^{13}\text{C}$ values between samples may be related to vent plume dynamics which are variable in space and time (Haalboom et al., 2020). The high correlation of $\delta^{13}\text{C}$ and relative TOC content in sediments (see Figure 5) suggests the input of fresh *in situ* derived organic carbon to the sediments near-vent and degradation with depth.

Off-vent, $\delta^{13}\text{C}$ sediment values were $\sim -21\text{‰}$ at the surface and $\sim -20\text{‰}$ at 5 cm core depth, pointing to a dominant input of photosynthetically derived OC from the surface ocean (~ -22 to -23‰). The discrepancy between $\delta^{13}\text{C}$ from surface waters and deep-sea sediments may be explained by a higher proportion of fresh, non-degraded algae, in the surface-waters. While sinking to 2000 m water depth, this algal material is reworked and mixed at the seabed with other carbon pools, which causes a positive shift in carbon isotopes. For instance, algal material being consumed by higher trophic levels would result in an increase of ~ 0.5 to 1‰ per trophic level (DeNiro and Epstein, 1981; Gearing, 1991).

The $\delta^{13}\text{C}$ values and TOC percentage in sediments reflect a mixture of different carbon sources for consumer communities, including fresh chemosynthetically-derived OC and photosynthetically derived OC from the surface ocean. Our data indicate that there is approximately 0.15% TOC in the open ocean sediment with a carbon isotope value of roughly -20.5‰ which represents photosynthetically derived OC. Close to the venting area, in addition to the photosynthetically derived carbon source, fresh *in situ* chemosynthetically derived OC is present, which is reflected by higher TOC and more depleted $\delta^{13}\text{C}$ values. Fauna close to vents uses this fresh organic matter as a food source. The contribution of chemosynthetic organic matter decreases with both sediment depth and distance from the vent (Figures 3, 4).

4.2 Chemosynthetic-Derived Organic Carbon as a Food Source for Fauna in Sediments

The $\delta^{13}\text{C}$ values of fauna near-vent ranged from ~ -25 to -28‰ and were similar to SPOM within the vent plume (-26‰ ; this study), suggesting selective feeding of (fresh) *in situ* derived organic carbon by near-vent fauna. The variability in stable isotope values may mirror the multiple chemosynthetic pathways of carbon production, such as methanotrophy versus autotrophy based on CBB or rTCA cycles according to the varying concentrations of reduced compounds (e.g. CH_4 , H_2S) at vent systems (Portail et al., 2018), as well as differences in the relative contribution of photosynthetic and chemosynthetic material at different sampling locations. The isotopic signatures from vent copepods (-26‰ to -29‰) from Portail's study were very similar to the isotopic signatures from copepods in this study living near-vent (-26‰), while the vent nematode signatures (-22‰ to -25‰) were less depleted than our near-vent nematodes (-28‰) (see Table 4).

The distinct $\delta^{13}\text{C}$ values of meiofauna near-vent (nematodes, copepods and polychaetes) suggest that these taxa may have different feeding strategies these groups may harbour several different species with different feeding strategies as well and/or ecological niches and rely on different food sources. Copepods and nematodes in sediments near-vent may selectively feed on chemosynthetic-derived organic carbon, similar to what was

TABLE 2 | Biomass of nematodes.

	Near-Vent (n= 417 ind.)	Off-Vent (n= 152 ind.)
Mean biomass of each individual (µg)	0.50 ± 3.93	0.93 ± 4.35
Mean length of each individual (µm)	713.95 ± 375.01	784.53 ± 759.20
Mean width of each individual (µm)	21.46 ± 9.91	25.77 ± 18.51

Mean and standard deviations of biomass, length and width of each individual, are provided for near-vent and off-vent.

TABLE 3 | Density of meiofauna from sediment samples.

Site	Year	Sample	SS	Total Area (cm ²)	Nematode density (10 cm ⁻²)	Copepod density (10 cm ⁻²)	Polychaete density (10 cm ⁻²)	Faunal density (10 cm ⁻²)
Near-Vent	2018	22BC	a+b+c	58.89	82.53	7.98	0	90.51
	2018	23BC	a	19.63	15.28	0.51	0	15.79
	2019	9BC	a+b+c	58.89	13.08	6.45	1.02	20.55
	2019	10BC	a+b+c	58.89	13.92	6.28	0.68	20.88
	2019	15BC	a+b+c	58.89	20.38	0.85	0.17	21.40
	2019	18BC	a+b+c	58.89	37.87	6.96	0.17	45.00
Mean					30.51	4.84	0.34	35.69
STD					27.11	3.28	0.42	28.78
Off-Vent	2018	11BC	a+b+c	58.89	20.55	4.58	0	25.13
	2018	12BC	a	19.63	23.94	1.02	0	24.96
	2018	13BC	a	19.63	13.75	1.02	0	14.77
	2019	13BC	a+b+c	58.89	50.94	2.72	0	53.66
	2019	14BC	a+b+c	58.89	45.68	7.30	0	52.98
	2019	19BC	a+b+c	58.89	24.11	3.57	0	27.68
Mean					29.83	3.37	0	33.20
STD					14.89	2.39	0	16.20

Site, year of sampling, name of sample (box corer), subsample (SS), total area of samples, mean density of nematode, copepod, polychaete individuals and total faunal density per 10 cm² are given.

observed for copepods in chimney-based sediments at vents near Japan (Nomaki et al., 2019). Less depleted polychaete δ¹³C signatures may point to a more mixed diet (photo- and chemosynthetically derived OC), a trophic increase, or a feeding niche in deeper sediment layers. However, Nomaki

et al. (2019) detected no depletion in nematodes near-vent, indicating that only copepods may selectively feed on organic matter produced through chemoautotrophy at the studied vent near Japan. In the RB sediments, nematodes showed high depletion and thus ingestion of *in situ* produced organic carbon.

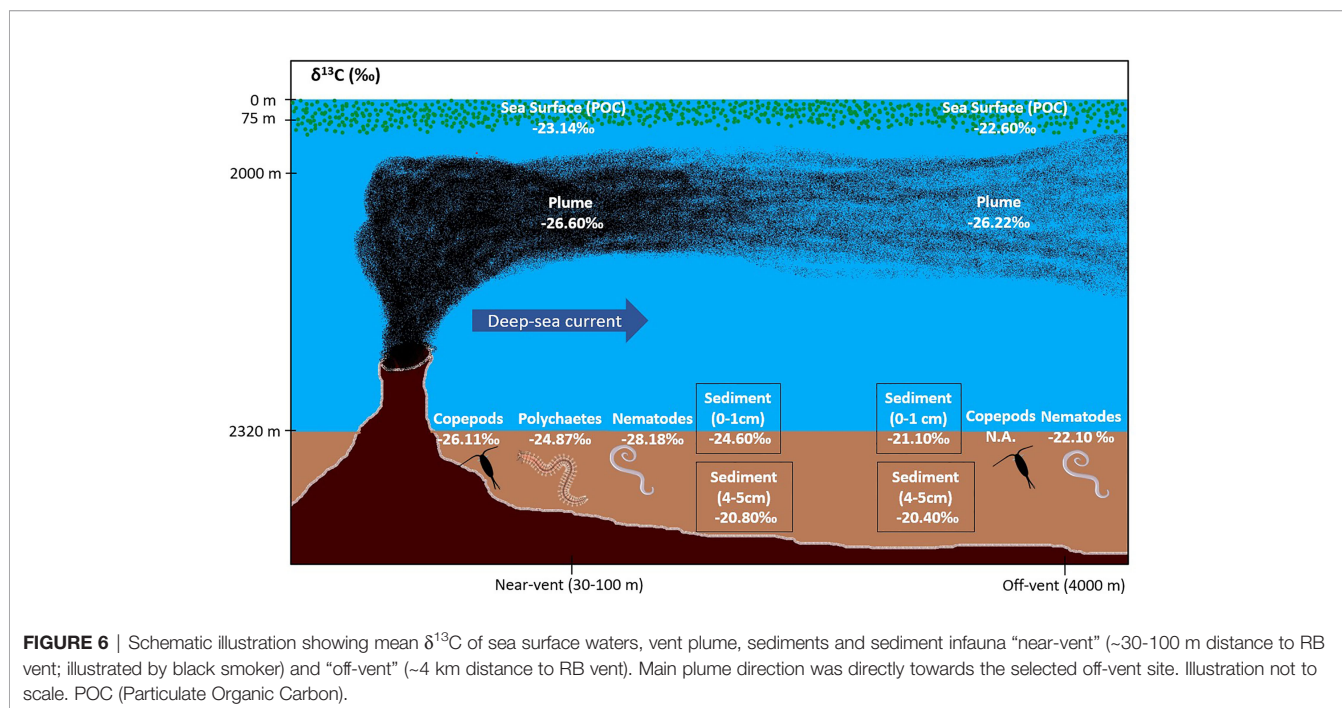


FIGURE 6 | Schematic illustration showing mean δ¹³C of sea surface waters, vent plume, sediments and sediment infauna “near-vent” (~30-100 m distance to RB vent; illustrated by black smoker) and “off-vent” (~4 km distance to RB vent). Main plume direction was directly towards the selected off-vent site. Illustration not to scale. POC (Particulate Organic Carbon).

TABLE 4 | $\delta^{13}\text{C}$ values of meiofauna from near-vent and off-vent measured in this study in comparison with other studies at and around the Rainbow vent field (MAR).

Location	At Vent			Near-vent			Off-vent	
Distance to vent (m)	0	0	0	185 to 370	< 50	30 to 100	13000	4000
Reference	Nomaki et al.	Alfaro-Lucas et al.	Portail et al.	Nomaki et al.	Alfaro-Lucas et al.	this study	Nomaki et al.	This study
Nematode	-26.61‰ & -23.24‰	-22.73‰	-25.30‰ to -22.80‰	-24.30‰	-23.30‰	-28.18‰	-23.40‰	-22.10‰
Copepod	-21.17‰ to -9.44‰	-34.57‰	-29.30‰ to -26.40‰	-21.30‰	-23.10‰	-26.11‰	-21.60‰	NA
Polychaete	-26.41‰ to -8.23‰	-31.47‰ to -21.69‰	-2.20‰ to -14.70‰	-20.50‰ & -20.10‰	-31.86‰ to -23.55‰	-24.87‰	NA	NA

NA, Not Available.

The $\delta^{13}\text{C}$ values of fauna off-vent were relatively similar to SPOM from the sea surface waters, suggesting that off-vent nematodes may feed on phytodetritus (Figure 6). Our findings are similar to the study of Nomaki et al. (2019), showing that fauna outside of the caldera and at caldera non-vent sites was less depleted in $\delta^{13}\text{C}$ relative to fauna at the base of the chimney (Table 4). A similar trend of decreasing depletion with distance from the active vents, although at a smaller scale (from at vent to 90 m to vent) was also observed for copepods at Lucky Strike (Alfaro-Lucas et al., 2020) (Table 4). Data thus suggest that the effect of *in situ* derived organic matter uptake by fauna may be limited to at most several 100 m (Nomaki et al., 2019). However, to precise the extent of influence of organic matter of chemosynthetic origin, future studies at RB vent field should consider samples between 100 and 4000 m distance from the vent.

4.3 Faunal Abundance and Biomass

The additional *in situ* derived food source (chemosynthetic OM) at near-vent did not result in enhanced overall abundance or biomass of nematodes, as similar abundance and biomass were observed near-vent and off-vent. Vanreusel et al. (2010) reviewed biomass data from nematodes living in chemosynthetic environments and showed that vent nematodes can be larger in comparison to reference sediments as an adaptation to low oxygen conditions (Vanreusel et al., 2010). In this study, nematodes' biomass (off-vent: 20.05 $\mu\text{gC } 10 \text{ cm}^{-2}$, near-vent: 30.68 $\mu\text{gC } 10 \text{ cm}^{-2}$) ranged in between the biomass of nematodes from two abyssal sites in the NE Atlantic in which one is oligotroph (EUMELI, 8.52 $\mu\text{gC } 10 \text{ cm}^{-2}$) and the other characterized by a high input of organic matter (Porcupine Abyssal Plain, 54.16 $\mu\text{gC } 10 \text{ cm}^{-2}$) (Vanreusel et al., 1995). Future studies should incorporate the abundance and biomass of all fauna in order to better understand the full impact of enhanced productivity on sediment communities near vents.

5 CONCLUSION

Our study shows that active vents are not isolated systems, but that *in situ* chemosynthetic-derived organic matter is traced back in the food web in near-vent areas. The degree of connection of

active vent ecosystems to their non-vent surroundings may depend on the direction, composition and volume of the vent plume. Future studies may explore in greater detail the change of food web and community structures along vent plume gradients and geographical distance to the active vent. Determining the true footprint of active vent systems is necessary in order to be able to determine the geographical size of any future area-based management tool.

DATA AVAILABILITY STATEMENT

The original contributions presented in the study are included in the article/Supplementary Material. Further inquiries can be directed to the corresponding author.

AUTHOR CONTRIBUTIONS

RR performed the stable isotope analyses, counted and identified animals, analyzed the data, and wrote the manuscript. RH analyzed nematode biomass. RB performed isotope analyses. MvM and FM advised on isotope and data analyses. SG designed the project, collected samples, and helped with data analyses. MvM, FM, and SG contributed to the writing and discussion. All authors contributed to the article and approved the submitted version.

FUNDING

We acknowledge the funding of the Netherlands Organisation for Scientific Research NWO and Royal Netherlands Institute for Sea Research NIOZ in organizing the Netherlands Initiative Changing Oceans NICO expedition in 2018. The study was supported by the following funds: "Erasmus+ Traineeship scholarship program of the University of Milan-Bicocca (to RR)", the Innovational Research Incentives Scheme of the Netherlands Organisation for Scientific Research (NWO) under grant agreement nos. 016.161.360 (to FM), the UU-NIOZ student work experience (to SG and Mei Nelissen), and the UU-NIOZ project "Protecting deep

seabed hydrothermal vent fields through area-based management tools”.

ACKNOWLEDGMENTS

We thank the captain and crew of RV Pelagia for their great support during expeditions. We further thank Rianna Vlierboom, Eva Paulus, and Mei Nelissen for support during research expeditions, for sorting fauna and preparing slides for

nematode analyses. We thank the reviewers and the editor for their very valuable comments to improve the quality of this manuscript.

SUPPLEMENTARY MATERIAL

The Supplementary Material for this article can be found online at: <https://www.frontiersin.org/articles/10.3389/fmars.2022.732740/full#supplementary-material>

REFERENCES

- Adams, D. K., Arellano, S. M., and Govenar, B. (2012). Larval Dispersal, Vent Life in the Water Column. *Oceanography* 25 (1), 255–685. doi: 10.5670/oceanog.2012.24
- Alfaro-Lucas, J. M., Pradillon, F., Zeppilli, D., Michel, L. N., Martinez-Arbizu, P., Tanaka, H., et al (2020). High Environmental Stress and Productivity Increase Functional Diversity Along a Deep-Sea Hydrothermal Vent Gradient. *Ecology* 101 (11), 1–13. doi: 10.1002/ecy.3144
- Andrassy, I. (1956). Die Rauminhalts-Und Gewichtsbestimmung Der Fadenwürmer (Nematoden). *Acta Zool. Hung.* 2.1, 1–5.
- Andreani, M., Ildefonse, B., Godard, M., and Escartin, J. (2014). Tectonic Structure, Lithology, and Hydrothermal Signature of the Rainbow Massif (Mid-Atlantic Ridge 36°14'N). *Geochem. Geophys. Geosyst.* 15 (9), 3543–3571. doi: 10.1002/2014GC005269.Received
- Bennett, S. A., Statham, P. J., Green, D. R.H., Le, N., Mcdermott, J. M., Prado, F., et al (2011). Deep-Sea Research I Dissolved and Particulate Organic Carbon in Hydrothermal Plumes From the East Pacific Rise, 9 1 50 0 NB. *Deep Sea Res. Part I* 58 (9), 922–315. doi: 10.1016/j.dsr.2011.06.010
- Boschen, R. E., Rowden, A. A., Clark, M. R., Barton, S. J., Pallentin, A., and Gardner, J. P. A. (2015). Megabenthic Assemblage Structure on Three New Zealand Seamounts: Implications for Seafloor Massive Sulfide Mining. *Mar. Ecol. Prog. Ser.* 523, 1–14. doi: 10.3354/meps11239
- Boschen, R. E., Rowden, A. A., Clark, M. R., and Gardner, J. P. A. (2013). Mining of Deep-Sea Seafloor Massive Sulfides: A Review of the Deposits, Their Benthic Communities, Impacts From Mining, Regulatory Frameworks and Management Strategies. *Ocean Coast. Manag.* 84, 54–67. doi: 10.1016/j.ocecoaman.2013.07.005
- Collins, P. C., Croot, P., Carlsson, J., Colaço, A., Grehan, A., Hyeong, K., et al. (2013). A Primer for the Environmental Impact Assessment of Mining at Seafloor Massive Sulfide Deposits. *Mar. Policy* 42, 198–209. doi: 10.1016/j.marpol.2013.01.020
- DeNiro, M. J., and Epstein, S. (1981). Influence of Diet on the Distribution of Nitrogen Isotopes in Animals. *Geochim. Cosmochim. Acta* 45 (3), 341–351. doi: 10.1016/0016-7037(81)90244-1
- Desbruyères, D., Caprais, M. B. J., Colaço, A., Comtet, T., Crassous, P., Fouquet, Y., et al (2001). Variations in Deep-Sea Hydrothermal Vent Communities on the Mid-Atlantic Ridge Near the Azores Plateau. *Dev. Hydrobiol.* 48, 1325–1346. doi: 10.1016/S0967-0637(00)00083-2
- Desbruyères, D., Sarradin, P. M., and Segonzac, M. (2000). A Review of the Distribution of Hydrothermal Vent Communities Along the Northern Mid-Atlantic Ridge: Dispersal vs. Environmental Controls 201–216. doi: 10.1007/978-94-017-1982-7_19
- Dover, C. L. V. (2011). Mining Seafloor Massive Sulphides and Biodiversity: What Is at Risk? *ICES J. Mar. Sci.* 68 (2), 341–348. doi: 10.1093/icesjms/fsq086
- Dover, C.L.V., Arnaud-Haond, S., Gianni, M., Helmreich, S., Huber, J. A., Jaeckel, A. L., et al (2018). Scientific Rationale and International Obligations for Protection of Active Hydrothermal Vent Ecosystems From Deep-Sea Mining. *Mar. Policy* 90, 20–28. doi: 10.1016/j.marpol.2018.01.020
- Dyment, J., Bissessur, D., Bucas, K., Cueff-Gauchard, V., Durand, L., Fouquet, Y., et al (2009). Detailed Investigation of Hydrothermal Site Rainbow, Mid-Atlantic Ridge, 36°13n: Cruise MoMARDream. *InterRidge News* 19, 22–24.
- Edmonds, H. N., and German, C. G. (2004). Particle Geochemistry in the Rainbow Hydrothermal Plume, Mid-Atlantic Ridge. *Geochim. Cosmochim. Acta* 68 (4), 759–25. doi: 10.1016/S0016-7037(03)00498-8
- Fry, B. (2006). *Stable Isotope Ecology* (New York, NY: Springer).
- Gearing, J. N. (1991). “The Study of Diet and Trophic Relationships Through Natural Abundance 13c.” in *Carbon Isotope Techniques*, vol. 201.
- German, C. R., Klinkhammer, G. P., and Rudnicki, M. D. (1996). The Rainbow Hydrothermal Plume, 36°15'N, MAR. *Geophys. Res. Lett.* 23 (21), 2979–2982. doi: 10.1029/96GL02883
- Giere, O. (2009). The Biotope: Factors and Study Methods,” in *Meiobenthology* Springer, Berlin, Heidelberg. doi: 10.1007/978-3-540-68661-3_2
- Gollner, S., Govenar, B., Arbizu, P. M., Mills, S., Le Bris, N., Weinbauer, M., et al (2015). Differences in Recovery Between Deep-Sea Hydrothermal Vent and Vent-Proximate Communities After a Volcanic Eruption. *Deep Sea Res. Part I Oceanogr. Res. Pap.* 106, 167–182. doi: 10.1016/j.dsr.2015.10.008
- Gollner, S., Govenar, B., Arbizu, P. M., Mullineaux, L. S., Mills, S., Le Bris, N., et al (2020). Animal Community Dynamics at Senescent and Active Vents at the 9° N East Pacific Rise After a Volcanic Eruption. *Front. Mar. Sci.* 6. doi: 10.3389/fmars.2019.00832
- Gollner, S., Kaiser, S., Menzel, L., Jones, D. O. B., Brown, A., Mestre, N. C., et al (2017). Resilience of Benthic Deep-Sea Fauna to Mining Activities. *Mar. Environ. Res.* 129, 76–101. doi: 10.1016/j.marenvres.2017.04.010
- Gollner, S., Riemer, B., Martínez Arbizu, P., le Bris, N., and Bright, M. (2010). Diversity of Meiofauna From the 9°50'N East Pacific Rise Across a Gradient of Hydrothermal Fluid Emissions. *PLoS One* 5 (8), e12321. doi: 10.1371/journal.pone.0012321
- Govenar, B. (2012). Energy Transfer Through Food Webs at Hydrothermal Vents Linking the Lithosphere to the Biosphere. *Oceanography* 25 (1), 246–255. doi: 10.5670/oceanog.2012.23
- Griffin, M. P. A., and Valiela, I. (2001). $\Delta^{15}\text{N}$ Isotope Studies of Life History and Trophic Position of *Fundulus heteroclitus* and *Menidia menidia*. *Mar. Ecol. Prog. Ser.* 214, 299–305. doi: 10.3354/meps214299
- Haalboom, S., Price, D. M., Mienis, F., Bleijswijk, J. D.L.V., De Stigter, H. C., Witte, H. J., et al (2020). Patterns of (Trace) Metals and Microorganisms in the Rainbow Hydrothermal Vent Plume at the Mid-Atlantic Ridge. *Biogeosciences* 17 (9), 2499–25195. doi: 10.5194/bg-17-2499-2020
- Higgins, R. P., and Thiel, H. (1988). *Introduction to the study of meiofauna*. (Smithsonian Institution Press).
- Holme, N. A., and McIntyre, A. D. (1971). *Methods for the Study of Marine Benthos*. Blackwell Scientific Publications.
- ISA (2019) “Guidance to Facilitate the Development of Regional Environmental Management Plans (REMPs)”. Available at: https://www.isa.org/im/files/files/documents/rempe_guidance_.pdf.
- Kendall, C., and Caldwell, E. A. (1998). Fundamentals of Isotope Geochemistry. In *Isotope tracers in catchment hydrology* (pp. 51–86). Elsevier. doi: 10.1016/B978-0-444-81546-0.50009-4
- Khripounoff, A., Vangriesheim, A., Crassous, P., Crassous, P., Segonzac, M., Colaço, A., et al (2001). Particle Flux in the Rainbow Hydrothermal Vent Field (Mid-Atlantic Ridge): Dynamics, Mineral and Biological Composition. *J. Mar. Res.* 59 (4), 633–656. doi: 10.1357/002224001762842217
- Kim, S. S. L., Mullineaux, L. S., and Helfrich, K. R. (1994). Larval Dispersal via Entrainment Into Hydrothermal Plumes Larval Dispersal via Entrainment Into Hydrothermal Vent Plumes. *J. Geophysical Res.: Oceans* 99 (C6), pp.12655–12665. doi: 10.1029/94JC00644

- Klunder, L., de Stigter, H., Lavaley, M. S. S., van Bleijswijk, J. D. L., van der Veer, H. W., Reichart, G. J., et al (2020). A Molecular Approach to Explore the Background Benthic Fauna Around a Hydrothermal Vent and Their Larvae: Implications for Future Mining of Deep-Sea SMS Deposits. *Front. Mar. Sci.* 7. doi: 10.3389/fmars.2020.00134
- Lebreton, B., Richard, P., Galois, R., Radenac, G., Brahmia, A., Colli, G., et al (2012). Food Sources Used by Sediment Meiofauna in an Intertidal *Zostera Noltii* Seagrass Bed: A Seasonal Stable Isotope Study. *Mar. Biol.* 159 (7), 1537–05. doi: 10.1007/s00227-012-1940-7
- Levin, L. A., Baco, A. R., Bowden, D. A., Colaco, A., Cordes, E. E., Cunha, M. R., et al (2016). Hydrothermal Vents and Methane Seeps: Rethinking the Sphere of Influence. *Front. Mar. Sci.* 3. doi: 10.3389/fmars.2016.00072
- Mattes, T. E., Nunn, B. L., Marshall, K. T., Proskurowski, G., Kelley, D. S., Kawka, O. E., et al (2013). Sulfur Oxidizers Dominate Carbon Fixation at a Biogeochemical Hot Spot in the Dark Ocean. *ISME J.* 7 (12) 2349–2360. doi: 10.1038/ismej.2013.113
- McCollom, T. M. (2000). Geochemical Constraints on Primary Productivity in Submarine Hydrothermal Vent Plumes. *Deep Sea Res. Part I Oceanogr. Res. Pap.* 47 (1), 85–101. doi: 10.1016/S0967-0637(99)00048-5
- Nomaki, H., Uejima, Y., Ogawa, N. O., Yamane, M., Watanabe, H. K., Senokuchi, R., et al (2019). Nutritional Sources of Meio- And Macrofauna at Hydrothermal Vents and Adjacent Areas: Natural-Abundance Radiocarbon and Stable Isotope Analyses. *Mar. Ecol. Prog. Ser.* 622, 49–65. doi: 10.3354/meps13053
- Pinnegar, J. K., and Polunin, N. V. C. (2000). Contributions of Stable-Isotope Data to Elucidating Food Webs of Mediterranean Rocky Littoral Fishes. *Oecologia* 122 (3), 399–4095. doi: 10.1007/s004420050046
- Portail, M., Brandily, C., Cathalot, C., Colaço, A., Gêlinas, Y., Husson, B., et al (2018). Food-Web Complexity Across Hydrothermal Vents on the Azores Triple Junction. *Deep Sea Res. Part I Oceanogr. Res. Pap.* 131, 101–120. doi: 10.1016/j.dsr.2017.11.010
- Spedicato, A., Sánchez, N., Pastor, L., Menot, L., and Zeppilli, D. (2020). Meiofauna Community in Soft Sediments at TAG and Snake Pit Hydrothermal Vent Fields. *Front. Mar. Sci.* 7. doi: 10.3389/fmars.2020.00200
- Thurnherr, A. M., and Richards, K. J. (2001). Hydrography and High-Temperature Heat Flux of the Rainbow Hydrothermal Site (36°14'N, Mid-Atlantic Ridge). *J. Geophys. Res. Oceans* 106 (C5), 9411–9426. doi: 10.1029/2000jc900164
- Thurnherr, A. M., Richards, K. J., German, C. R., Lane-Serff, G. F., and Speer, K. G. (2002). Flow and Mixing in the Rift Valley of the Mid-Atlantic Ridge 1763–1778. doi: 10.1175/1520-0485(2002)032%3C1763:FAMITR%3E2.0.CO;2
- Vanreusel, A., De Groot, A., Gollner, S., and Bright, M. (2010). Ecology and Biogeography of Free-Living Nematodes Associated With Chemosynthetic Environments in the Deep Sea : A Review. *PLoS One* 5 (8), e12449. doi: 10.1371/journal.pone.0012449
- Vanreusel, A., Vincx, M., Bett, B. J., and Rice, A. L. (1995). Nematode Biomass Spectra at Two Abyssal Sites in the NE Atlantic With a Contrasting Food Supply. *Int. Rev. Ges. Hydrobiol. Hydrogr.* 80 (2), 287–965. doi: 10.1002/iroh.19950800215

Conflict of Interest: The authors declare that the research was conducted in the absence of any commercial or financial relationships that could be construed as a potential conflict of interest.

Publisher's Note: All claims expressed in this article are solely those of the authors and do not necessarily represent those of their affiliated organizations, or those of the publisher, the editors and the reviewers. Any product that may be evaluated in this article, or claim that may be made by its manufacturer, is not guaranteed or endorsed by the publisher.

Copyright © 2022 Roohi, Hoogenboom, Van Bommel, Van Der Meer, Mienis and Gollner. This is an open-access article distributed under the terms of the Creative Commons Attribution License (CC BY). The use, distribution or reproduction in other forums is permitted, provided the original author(s) and the copyright owner(s) are credited and that the original publication in this journal is cited, in accordance with accepted academic practice. No use, distribution or reproduction is permitted which does not comply with these terms.